$NaHCO_3$ (pH=7), and suspended by magnetically stirring. Then, CO_2 was bubbled into the solution at a flow rate of 30 mL min^{-1} without irradiation for 1.5 hours. The photocatalytic reaction was conducted using a 100 W high-pressure mercury lamp. The light intensity was measured to be 22 mW cm^{-2} at a detecting wavelength of 254±10nm. The reaction temperature was set at 290 K with cooling water. The amount of the products (H_2, O_2, and CO) in the outlet gas from the reactor were determined by using an on-line gas chromatograph (Shimadzu, GC-8A, TCD, a Shincarbon ST column, argon carrier).

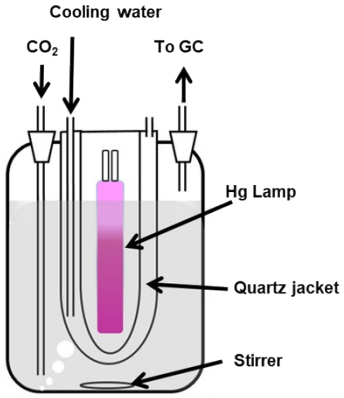

Fig. S1 The reactor set-up for the photocatalytic reaction test for CO_2 reduction with water under photoirradiation.

2. Results

2.1. XRD and SEM image of potassium hexatitanate

Fig.S2 shows XRD patterns of the obtained KTO sample and a $K_2Ti_6O_{13}$ reference from a database (ICSD#25712). The XRD pattern of the prepared KTO sample was consistent with that of the reference. It gives a correct diffraction pattern and no diffraction lines corresponding to other impurity phases, confirming that the prepared potassium hexatitanate was correctly fabricated by the flux method.

Fig.S3 shows that the KTO sample consisted of rod-like crystals with similar morphology and size.

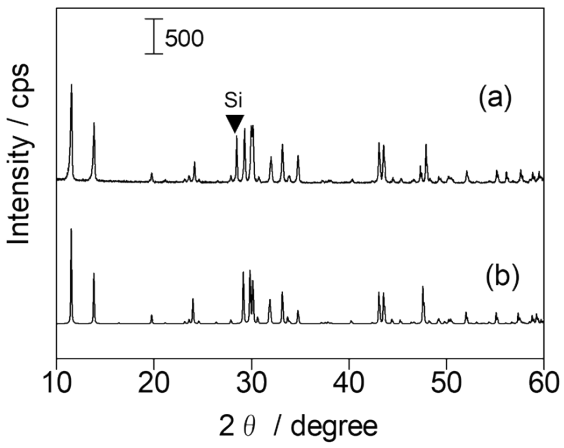

Fig. S2 XRD patterns of (a) the prepared KTO sample and (b) a reference data #25712 from ICSD database for $K_2Ti_6O_{13}$. A closed triangle indicates a diffraction from silicon powder mixed with the KTO sample to calibrate the angle.

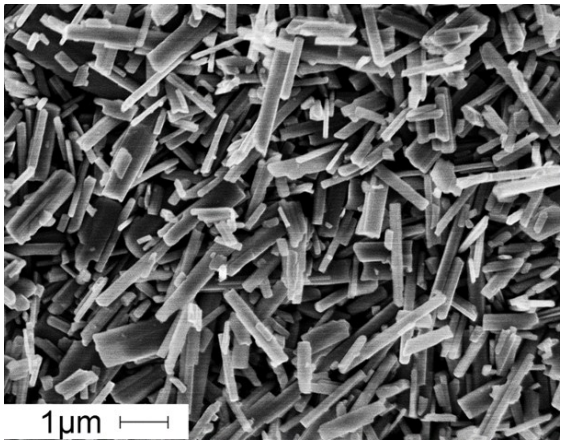

Fig. S3 SEM image of the prepared KTO sample.

2.2. Photocatalytic reaction tests

The results of photocatalytic reaction tests over eight samples loaded with different cocatalysts were shown in Fig. S4. The Ag(1.0)/KTO sample produced CO with high selectivity (S_{CO}=94.8%). The samples with the Ag-Pd, Ag-Au, or Ag-Cu dual cocatalyst produced H_2 preferably, and other samples with the Ag-Cr, Ag-Ni, Ag-Co, or Ag-Mn dual cocatalyst formed predominantly CO with high selectivity more than 85%. As was well known, the precious metal cocatalysts, such as Pd and Pt cotatalyst,[4] are very beneficial to the H_2 evolution, while the transition metal oxide cocatalysts such as MnO_x and CrO_x exhibit high activity for O_2 evolution.[5] In the current study, the photocatalyst with a Ag-MnO_x dual cocatalyst exhibited the highest activity than other dual cocatalysts. In the present study the cocatalysts were loaded by a photodeposition method and the real loading amount of CrO_x, CoO_x and NiOx were very limited. Thus, the deposition method and the amount of cocatalysts deposited are supposed to the possible reasons for low activity. This remains further possibilities that other transition metal oxide species might exhibit high performance after each optimization.

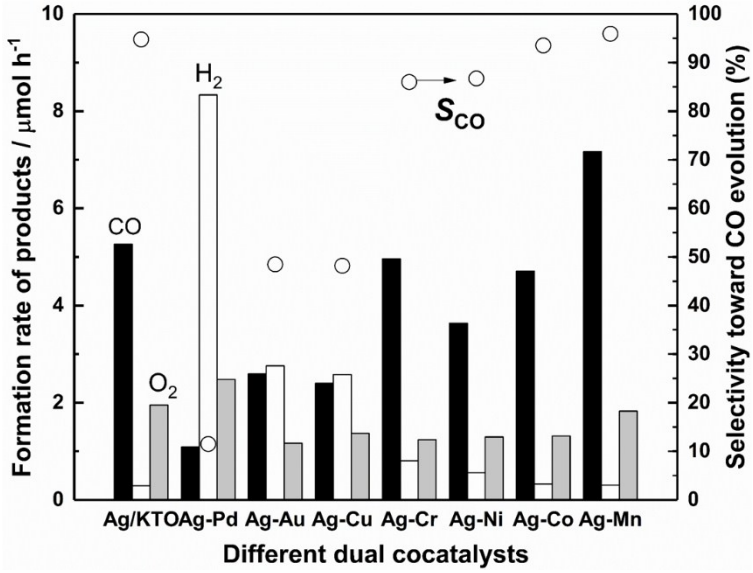

Fig. S4 Formation rates of CO (black bar), H_2 (white bar), and O_2 (grey bar) and the S_{CO} (open circles) in the photocatalytic CO_2 reduction with H_2O over the prepared KTO samples, (a) Ag(1.0)/KTO, (b) Ag(1.0)-Pd(1.0)/KTO, (c) Ag(1.0)-Au(0.85)/KTO, (d) Ag(1.0)-Cu(1.0)/KTO, (e) Ag(1.0)-Cr(0.006)/KTO, (f) Ag(1.0)-Ni(0.02)/KTO, (g) Ag(1.0)-Co(0.02)/KTO, and (h) Ag(1.0)-Mn(0.09)/KTO.

The photocatalytic reaction tests were conducted for the Ag-Mn/KTO samples with different Ag loading amount (Fig. S5). Although the same amount of Mn was added, the actually loaded amount of Mn was varied with the loading amount of Ag cocatalyst. It was found that the formation rate of CO first increased then decreased with the increasing loading amount of Ag cocatalyst. The samples with moderate loading amount in the range of 0.5–2.0 wt% of Ag and 0.10-0.13 wt% of Mn (Fig. S5, e–g) exhibited high photocatalytic activity for CO evolution. When the Ag loading amount is more than 2 wt%, the Ag particles would aggregate and the photocatalytic activity of CO_2 reduction would decrease.

Some blank tests were carried out by using the Ag(0.5)-Mn(0.13)/KTS sample as shown in Table S1. No product was detected under dark conditions (Table S1, entry 2). Without a photocatalyst or without using a $NaHCO_3$ additive, only very low amounts of CO and H_2 were obtained (Table S1, entries 3 and 4), indicating that the photocatalyst and $NaHCO_3$ were both necessary to yield them sufficiently. And when a flow of argon gas was used instead of the flowing CO_2 gas (Table S1, entry 5), the CO evolution was also observed since CO_2 is formed from $NaHCO_3$ in the solution due to the equilibrium, but the rate was quite low, showing the predominant CO formation originates from molecular CO_2.

Table S1 Results of some blank tests for the photocatalytic CO_2 reduction with H_2O under different conditions.

Entry	conditions	Formation rate of products / μmol h^{-1}			S_{CO}(%)[b]
		CO	H_2	O_2	
1	standard conditions[a]	10.07	0.20	4.39	98.2
2	without irradiation	0.00	0.00	0.00	–
3	without photocatalyst	0.81	0.91	0.17	47.1
4	without $NaHCO_3$	0.99	0.75	0.00	56.9
5	without CO_2	1.63	0.19	0.75	89.6

[a] Photocatalyst the Ag(0.5)-Mn(0.13)/KTS sample, 0.3 g, reaction solution volume: 0.4 L, additive: 0.5 M $NaHCO_3$, CO_2 flow rate: 30 mL min^{-1}, light source: a 100 W high pressure Hg lamp. [b] Selectivity to CO, $S_{CO}(\%) = 100 \times R_{CO} / (R_{CO} + R_{H2})$, where R_{CO} and R_{H2} are the production rate of CO and H_2, respectively.

The recycle tests were performed to confirm the stability and durability of the prepared sample repeatedly for two time under the same conditions. The first run is shown in Fig.1 and the second one (reused test) is presented below as Fig. S7. Also in the second run, almost the same formation rates of CO and H_2 were achieved, while there was a slight loss by a ca. 10% O_2 evolution activity. This may due to the ca. 15% loss of both Ag and MnO_x cocatalyst, which was confirmed by the XRF.

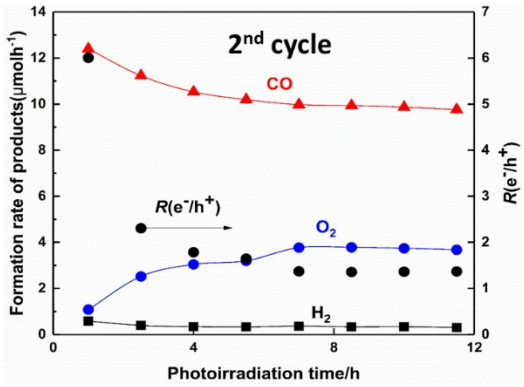

Fig. S7 Time course of the production rates of CO, H_2, and O_2, and R(e^-/h^+) with the Ag(0.5)-Mn(0.13)/KTS sample in the photocatalytic CO_2 reduction test as the second run after the first run shown in Fig.1.

2.5. SEM images and TEM-EDS mappings

The SEM images of the prepared Ag(1.0)/KTO and Ag(1.0)-Mn(0.09)/KTO samples were shown in Fig. S11. The Ag nanoparticles loaded on the Ag(1.0)/KTO sample were clearly observed. Nanoparticles were also observed for the Ag(1.0)-Mn(0.09)/KTO samples, although it is very hard to distinguish the Ag cocatalyst and MnO_x cocatalyst.

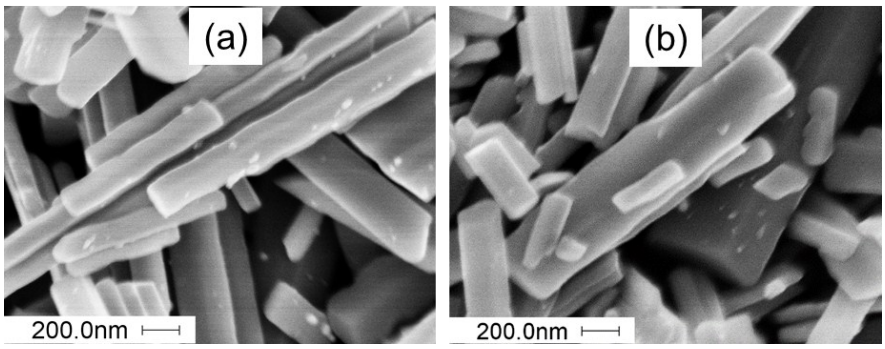

Fig. S11 SEM images of (a) the Ag(1.0)/KTO sample, and (b) the Ag(1.0)-Mn(0.09)/KTO sample.

Fig. S12a and S12b show the TEM images of the prepared Ag(1.0)/KTO and Ag(1.0)-Mn(0.09)/KTO samples, respectively, where nanoparticles were observed on the surface of these two samples. As confirmed by EDS mappings shown at the right side of TEM images, the observed nanoparticles were assignable to Ag nanoparticles. Although some dots were found in each EDS mapping of Mn, they were assignable to not Mn species but the background noise because these dots are observed even in the area without any material, i.e., upper side in Fig. S12(a) and upper middle area in Fig. S12(b). Therefore, the Mn species were not confirmed by the EDS mapping for both the Ag(1.0)/KTO and Ag(1.0)-Mn(0.09)/KTO samples, which may be due to the extremely low concentration as well as the amorphous and well dispersed structure.

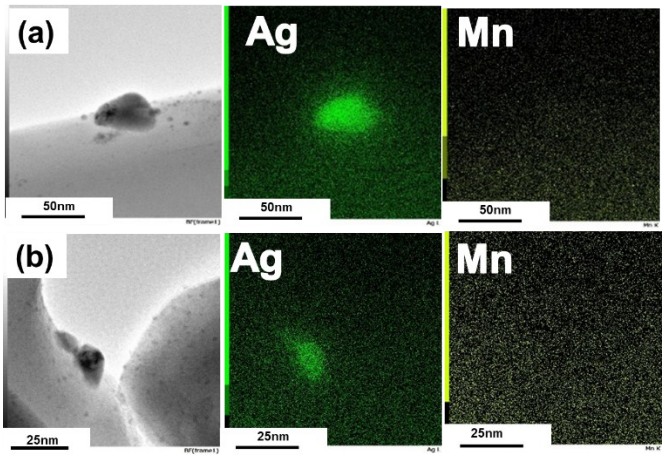

Fig. S12 TEM images and EDS mappings of (a) the Ag(1.0)/KTO sample, and (b) the Ag(1.0)-Mn(0.09)/KTO sample.

Table S2 shows the comparison of CO formation rate and selectivity for photocatalytic CO_2 reduction with H_2O in reported researches, although the reaction conditions were quite different from each other, for example using a large scale reactor, a high-powered lamp, and a large amount of water and photocatalyst. Among them, the current photocatalytic system shows a moderate activity and the highest selectivity.

Table S2 Reported photocatalytic performances in photocatalytic CO_2 reduction with H_2O.

Entry	Photocatalyst	Weight of sample (g)	Volume of water (L)	High pressure mercury Lamp (W)	CO evolution activity (μmol h^{-1})	CO selectivity (%)
1[6a]	$Ag/BaLa_4Ti_4O_{15}$	0.3	0.36	400	22	67
2[6b]	$Ba_2Li_{2/3}Ti_{16/3}O_{13}$	1.0	1.8	400	1.6	12
3[6c]	$Ag/SrNb_2O_6$	0.5	1.0	400	36	96
4[6d]	$Ag/ZnGa_2O_4/Ga_2O_3$	1.0	1.0	400	108	92
5[1a]	$Ag/Na_2Ti_6O_{13}$	0.3	0.35	100	2.8	82
6 (Current study)	$Ag\text{-}Mn/K_2Ti_6O_{13}$	0.3	0.4	100	10	98

References

1 (a) X. Zhu, A. Anzai, A. Yamamoto and H. Yoshida, Appl. Catal. B Environ., 2019, 243, 47. (b) H. Yoshida, M. Sato, N. Fukuo, L. Zhang, T. Yoshida, Y. Yamamoto, T. Morikawa, T. Kajino, M. Sakano, T. Sekito, S. Matsumoto, H. Hirata, Catal. Today, 2017, 303, 296.

2 R. Pang, K. Teramura, H. Tatsumi, H. Asakura, S. Hosokawa and T. Tanaka, Chem. Commun., 2018, 54, 1053.

3 A. Anzai, N. Fukuo, A. Yamamoto and H. Yoshida, Catal. Commun., 2017, 100, 134.

4 (a) Y. Ma, R. Chong, F. Zhang, Q. Xu, S. Shen, H. Han and C. Li, Phys. Chem. Chem. Phys., 2014, 16, 17734. (b) R. Pang, K. Teramura, H. Tatsumi, H. Asakura, S. Hosokawa and T. Tanaka, Chem. Commun., 2018, 54, 1053.

5 (a) J. Yang, D. Wang, H. Han and C. Li, Acc. Chem. Res., 2013, 46, 1900. (b) R. Li, F. Zhang, D. Wang, J. Yang, M. Li, J. Zhu, X. Zhou, H. Han and C. Li, Nat. Commun., 2013, 4, 1432.

6 (a) K. Iizuka, T. Wato, Y. Miseki, K. Saito and A. Kudo, J. Am. Chem. Soc., 2011, 133, 20863. (b) L. F. Garay-Rodríguez, H. Yoshida, and L. M. Torres-martínez, Dalton Trans., 2019, 48, 12105. (c) R. Pang, K. Teramura, H. Asakura, S. Hosokawa and T. Tanaka, Appl. Catal. B Environ., 2017, 218, 770. (d) Z. Wang, K. Teramura, Z. Huang, S. Hosokawa, Y. Sakata and T. Tanaka, Catal. Sci. Technol., 2016, 6, 1025.